Chapter 4
Physical Vibration Simulation of an Acoustic Environment with Six Shakers on an Industrial Structure

Randall L. Mayes and Daniel P. Rohe

Abstract A previous study in the UK demonstrated that vibration response on a scaled-down model of a missile structure in a wind tunnel could be replicated in a laboratory setting with multiple shakers using an approach dubbed as impedance matching. Here we demonstrate on a full scale industrial structure that the random vibration induced from a laboratory acoustic environment can be nearly replicated at 37 internal accelerometers using six shakers. The voltage input to the shaker amplifiers is calculated using a regularized inverse of the square of the amplitude of the frequency response function matrix and the power spectral density responses of the 37 internal accelerometers. No cross power spectral density responses are utilized. The structure has hundreds of modes and the simulation is performed out to 4000 Hz.

Keywords MIMO shaker control • Multi-shaker simulation

Nomenclature

ω	Frequency in radians per second
$+$	Superscript indicating the Moore-Penrose pseudo-inverse of a matrix
c	Tikhonov regularization constant
d	Subscript for desired value
DFAT	Direct field acoustic test
dof	Degree of freedom
FRF	Frequency response function
H	Frequency response function matrix
i	Subscript for initial value
IMMAT	Impedance matched multi-axis testing
MIMO	Multi-input multi-output
PSD	Power spectral density
RMS	Root mean square
S	Absolute value of FRF matrix squared element by element
v	Voltage
x	Physical displacement dof

4.1 Introduction and Motivation

Most engineering laboratories understand that ground based testing of systems on shaker tables has serious shortcomings when compared with the true environment of a payload. A few of these limitations are:

Sandia National Laboratories is a multi-program laboratory managed and operated by Sandia Corporation, a wholly owned subsidiary of Lockheed Martin Corporation, for the U.S. Department of Energy National Nuclear Security Administration under Contract DE-AC04-94AL85000.

R.L. Mayes (✉) • D.P. Rohe
Structural Dynamics, NDE and Model Validation Department, Sandia National Laboratories, Albuquerque, NM 87185, USA
e-mail: rlmayes@sandia.gov; dprohe@sandia.gov

A. Brandt, R. Singhal (eds.), *Shock & Vibration, Aircraft/Aerospace, Energy Harvesting, Acoustics & Optics, Volume 9*,
Conference Proceedings of the Society for Experimental Mechanics Series, DOI 10.1007/978-3-319-30087-0_4

1. The shaker table can only excite the payload in one single axis at a time, so at least three tests have to be performed to capture the three dimensional aspects of the field vibration;
2. The impedance of the shaker table is radically different from the parent structure supporting the payload;
3. Forces are often coming into the payload at multiple points in the true environment, and these effects cannot be simulated with a shaker table;
4. These shortcomings often result in severe overtests for many frequency bands as well as undertests [1] in other bands.

The problems are amplified if one is attempting to simulate vibration that is partially or completely caused by aerodynamic forces on the payload. Theoretically, one does not have to excite a payload with exactly the same loadings as it sees in the operational environment. If enough shakers can be placed at proper locations on the structure and controlled to excite it with the same modal forces, it should see exactly the same vibrational response. There are an infinite number and combination of locations that shakers could be attached to excite the same modal forces as the operational environment. The work in this paper was actually proposed four years ago, but just recently came to fruition. Daborne, et al. presented an approach to the problem [2] and a review of the problem and a successful testing solution [3] on a 1/3 scale model of an underwing missile. In their demonstration, the operational environment of the scale model missile attached to its carriage fixture was generated in a wind tunnel and measured with 13 accelerometers. Then in the vibration laboratory, the missile was mounted to its underwing carriage on a board and excited with three shakers. They achieved an excellent match to the cross power spectral density matrix for all 13 accelerometers with a multiple input multiple output (MIMO) control system. The method was dubbed Impedance Matched Multi-Axis Testing (IMMAT).

Here we attempt to provide a similar demonstration on an industrial payload supported by a mounting rack. The environment is generated acoustically with eight drives for a large system of speakers in the truth test. Then the payload is suspended on its rack with bungee cords, and six shakers are driven to attempt to reproduce the internal vibration of the truth acoustic environment in a modal test lab. Thirty seven internal accelerometers are the target responses. There are hundreds of modes in the 4000 Hz bandwidth. This work focuses on reproducing the accelerometer power spectral densities and does not require cross spectral densities.

In Sect. 4.2 the test hardware and instrumentation is described. Section 4.3 provides the description of the acoustic truth test. Section 4.4 describes the multi-shaker simulation which attempts to reproduce the vibration response of the acoustic truth test. In Sect. 4.5 the theory is explained for generating the proper shaker amplifier input voltages to perform the simulation. Sections 4.6 and 4.7 address some logistic details for a multi-shaker simulation and in Sect. 4.8 conclusions are provided.

4.2 Test Hardware and Instrumentation

The industrial structure of interest is shown in Fig. 4.1 in one of several test setups. The structure was attached to a supporting rack from which it hung. The structure has hundreds of modes up to the desired bandwidth of 4000 Hz. There are dozens of instrumented components inside the structure. For this work 37 internal accelerometers were selected as those of primary interest. In addition there were several dozen accelerometers that were monitoring response on the external skin and on the rack. Most of the accelerometers were of the integrated circuit piezoelectric type with 10 mv/G sensitivity. All data were acquired using IDEAS software for the acoustic test and the later vibration simulation tests. VTI 1436 modules were utilized to acquire the data and VTI 1434 source modules were used to provide either flat random voltage inputs for frequency response function (FRF) calculations or prescribed user defined voltage time histories to excite the required response. For the vibration test of interest six MB 50 shakers with Yamaha model P7000S amplifiers were used to excite the structure. Bungee cords supported the rack and structure.

In Fig. 4.2 one can see three shakers attached to the supporting rack with their connecting hardware. Steel rods of about 1.6 mm diameter and about 25 mm length are used to minimize transmission of moments and shear forces from the shaker to the test article. Drive point accelerometers are utilized, and they are covered with an aluminum cap to which the force gage is mounted. Aluminum receptacles attach the stinger to the force gage and also to the shaker. Set screws hold the steel rods in the aluminum receptacles.

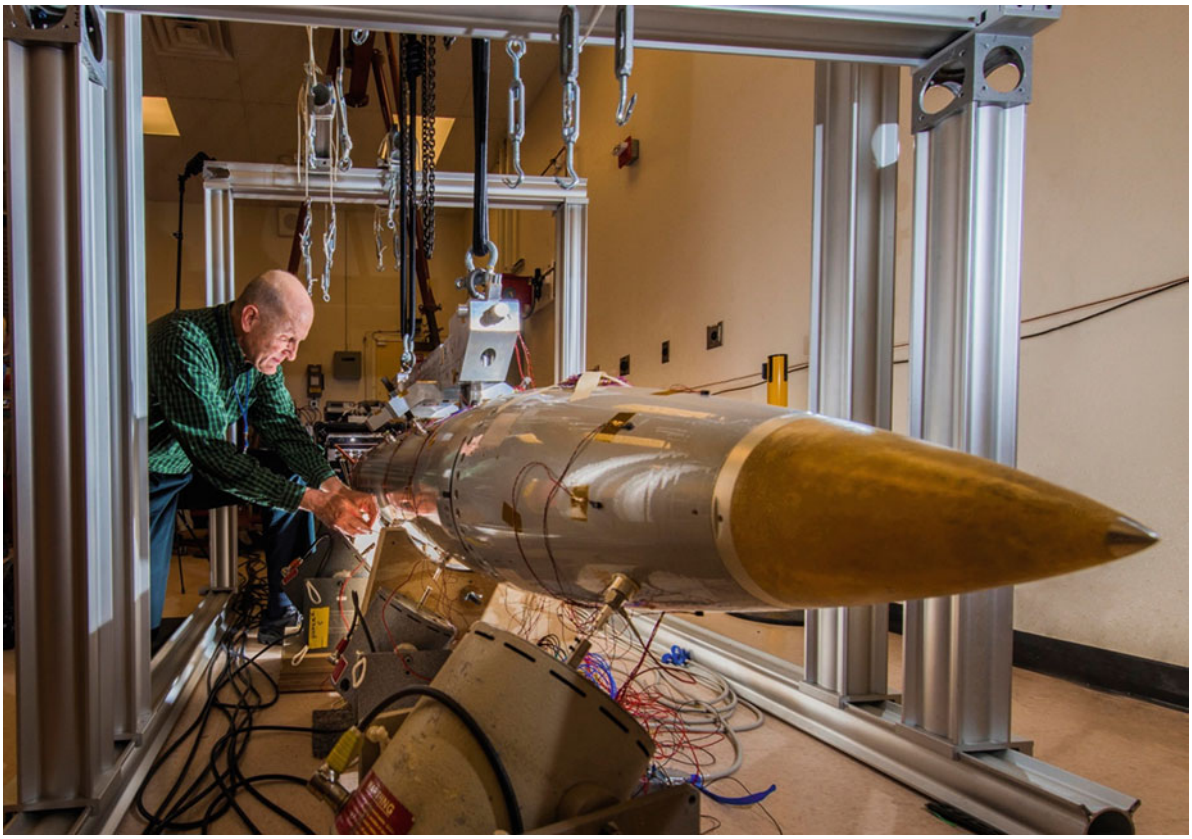

Fig. 4.1 Industrial structure mounted on support rack in one test configuration

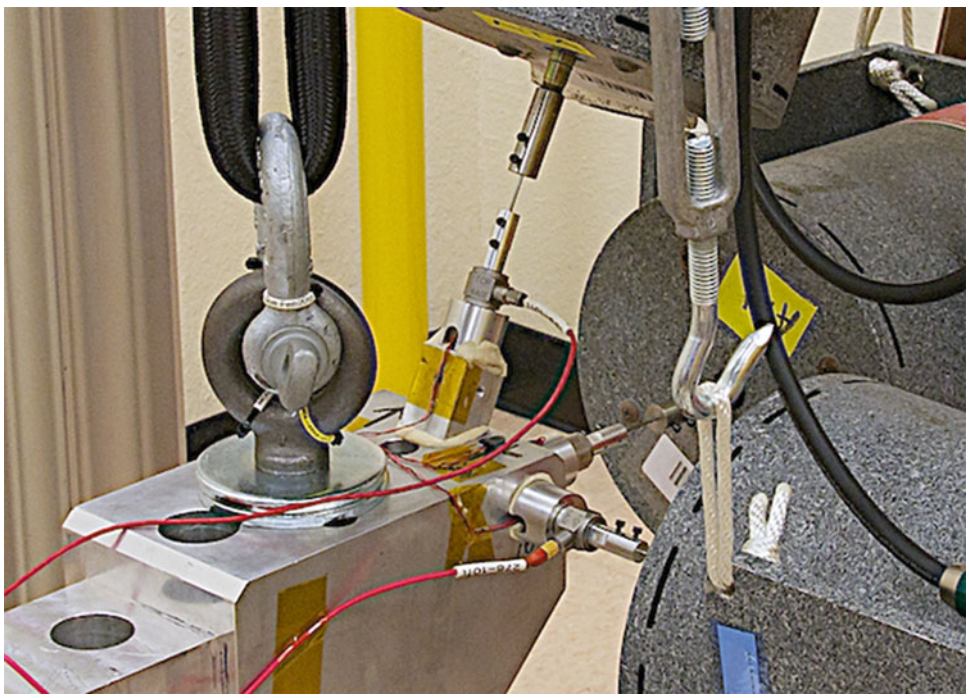

Fig. 4.2 Shaker attachment hardware

4.3 Acoustic "Truth" Test

The acoustic test setup is shown in Fig. 4.3. This serves as our "truth" test, or the actual environment for this research. The test was performed at the Sandia National Laboratories acoustic test facility with the direct-field acoustic test (DFAT) approach. Twelve VT-99 model speaker cabinets and six low frequency model VS-Q speakers surround the test article in eight speaker stacks. Multiple Input Multiple Output (MIMO) control was accurately maintained at the six control microphones. All six microphones had the same flat topped drive specification with 0.1 coherence between microphones. The drive levels were at the limits of speaker/amplifier capability. Dozens of accelerometers were mounted on the skin, rack and yoke and dozens more were on internal components. Twelve other response microphones were also placed around the unit. The industrial test structure was supported on its rack with a large yoke made of steel bars, which allowed the structure to be suspended and rotated into a vertical position to facilitate the placement of speakers radially around it. (The rack is not visible in this view, but the steel bars of the yoke are visible).

4.4 MIMO Simulation Test

The MIMO shaker simulation test was set up in a modal testing laboratory at Sandia National Laboratories. The rack and industrial structure were suspended as shown in Fig. 4.1. Several different shaker arrangements were executed for various purposes not germane to this paper. The MIMO simulation configuration was chosen based on information gained from these configurations.

4.4.1 MIMO Simulation Test Setup

The MIMO simulation configuration had two floor mounted shakers attached to the belly of the industrial structure, and four attached to the rack. Two lateral shakers were attached near the forward and aft ends of the rack and two more vertically oriented shakers were attached at the forward and aft ends of the rack. The vertical shakers had a 21.5° tilt from vertical simply to keep the shaker from interfering with the bungee cord support. (See the vertical shaker in Fig. 4.2). Flat random voltage inputs which produced about 45 N RMS force from 25 to 4000 Hz were utilized to calculate accelerometer response to input voltage FRFs for the six shaker drives. One hundred averages were used with a frequency resolution of 2.5 Hz. These FRFs were used to back calculate input voltages to drive the shakers to attempt to produce the same accelerometer power spectral densities (PSDs) as were measured in the acoustic "truth" test. The simulation was adjusted in steps with three iterations to the final physical simulation. 37 internal accelerometers were chosen as accelerometers of interest for which the shaker simulation attempted to match the acoustic test PSDs.

4.4.2 MIMO Simulation Test Results

A metric which provides a single plot comparison of the overall match of the simulation was the sum of the 37 PSDs. This sum of PSDs for the acoustic test (blue) and the vibration test (red) is shown in Fig. 4.4. For most of the band, the vibration test closely envelopes the acoustic test. The band from 3500 to 4000 Hz does not match near as well as the rest of the frequency range. In Fig. 4.5 is shown a couple of the PSDs from individual accelerometers that gives an indication of the "best" and "worst" gage responses. In the worst gage, there are several bands where the vibration test overshoots the desired PSD. These results are very encouraging, and the vibration simulation with six shakers is certainly much better than could be obtained by setting the unit on a shaker table and attempting to control all 37 gages.

There was a portion of the structure that had some intermittent nonlinearity. In Fig. 4.6 one can see the PSD of an accelerometer in this region. The plot shows the truth test result that we desire to match in blue. The red plot shows one physical vibration simulation measurement and the magenta plot shows another physical vibration simulation where everything in the vibration test was repeated exactly as before. The nonlinearity is intermittent.

Fig. 4.3 Acoustic “Truth” test setup

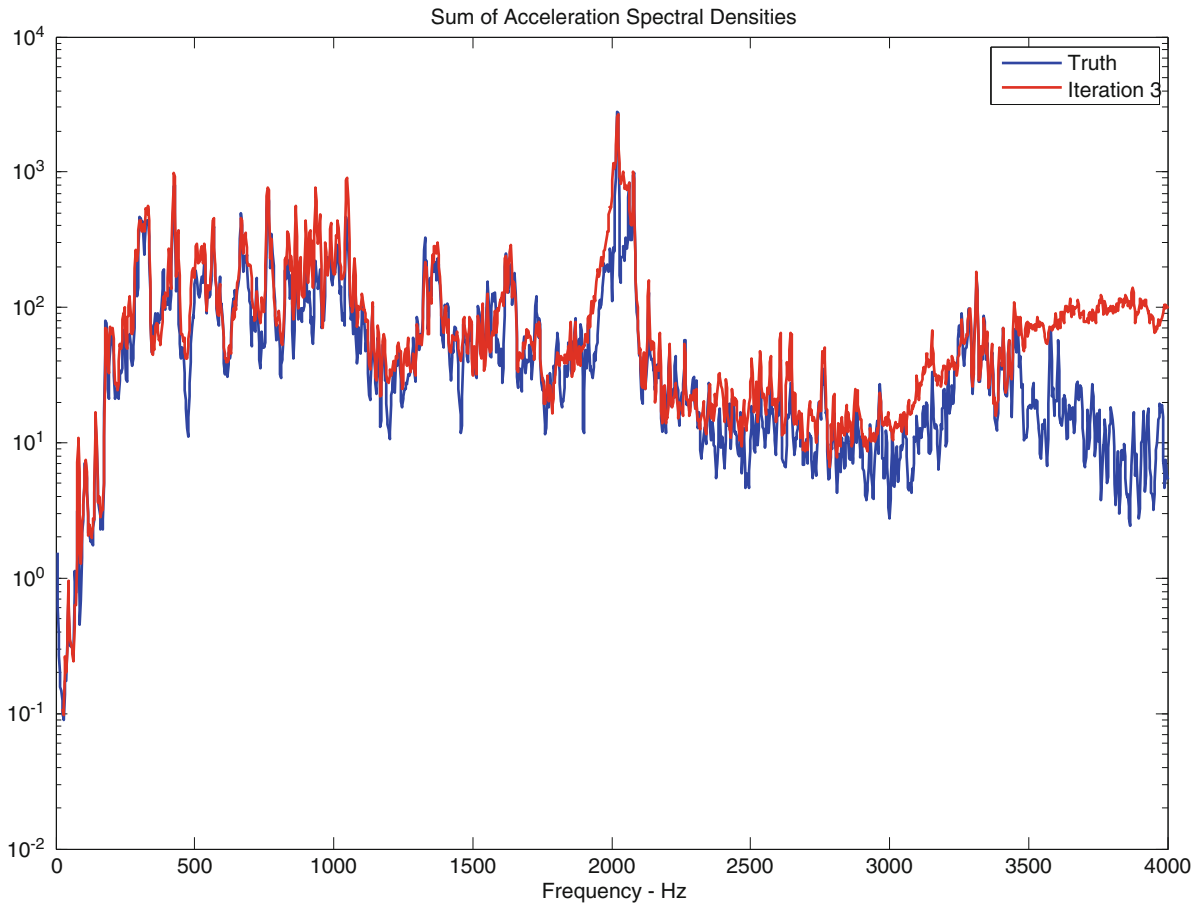

Fig. 4.4 Comparison metric (Sum of PSDs) for 37 accelerometers for the acoustic test (*blue*) and 6 shaker vibration test (*red*)

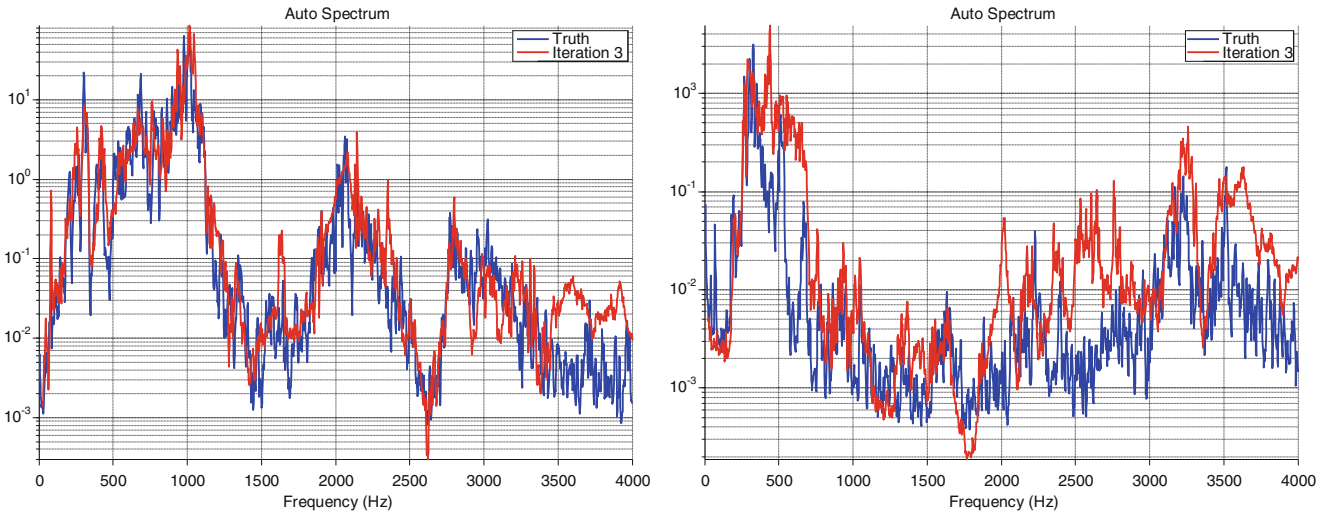

Fig. 4.5 Individual acceleration spectral density—best (*left*) and worst (*Right*) comparisons of acoustic test (*blue*) and vibration test (*red*)

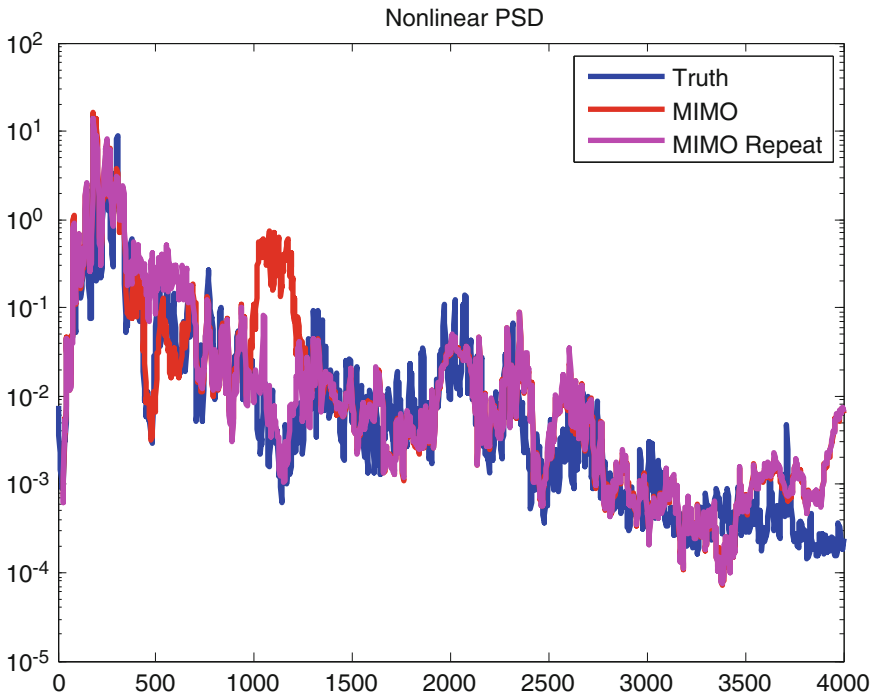

Fig. 4.6 PSD with intermittent nonlinearity—acoustic test (*blue*). Vibration test (*red*)—repeat of vibration test (*magenta*)

4.5 Simulation Theory

For a linear system, the relationship between input voltage to a set of shaker amplifiers and the output response acceleration at many degrees of freedom (dof) can be given as

$$\overline{\ddot{x}}(\omega) = \mathbf{H_{xv}}(\omega)\overline{v}(\omega) \tag{4.1}$$

where ω specifies each frequency line, $\overline{\ddot{x}}$ specifies acceleration at instrumented locations, **H** is matrix of frequency response functions and vector v is the input voltage. Assuming that the calculation is made for each frequency line, let us drop the omega term for convenience. It can be shown for uncorrelated voltage inputs that the autospectra of the responses is the magnitude squared of the FRF matrix times the autospectra of the input voltages, or

$$\left|\overline{\ddot{x}}\right|.^{\wedge 2} = |\mathbf{H_{xv}}|.^{\wedge 2} * |\overline{v}|.^{\wedge 2} \tag{4.2}$$

where .^ denotes element-wise exponentiation.

Define matrix **S** as

$$\mathbf{S} = |\mathbf{H_{xv}}|.^{\wedge 2} \tag{4.3}$$

To correct for ill-conditioning of **S**, use the Tikhonov regularization to adjust the Moore-Penrose pseudo-inverse as

$$\mathbf{S}^{+} = \left[\mathbf{S}^{T} * \mathbf{S} + c * \mathbf{I}\right]^{-\mathbf{1}} * \mathbf{S}^{T} \tag{4.4}$$

so an estimate of the voltage autospectra is the Tikhonov pseudo-inverse of the squared FRF matrix times the autospecra of the target accelerometers

$$|\overline{v}|.^{\wedge 2} = \mathbf{S}^{+} * \left|\overline{\ddot{x}}\right|.^{\wedge 2} \tag{4.5}$$

To handle some mild nonlinearity, after each iteration one calculates the change in voltage needed to create an appropriate change in autospectrum of the accelerations and simply adds that to the last voltage autospectrum (subscript i here).

$$|\overline{v}_d|.^{\wedge 2} = |\overline{v}_i|.^{\wedge 2} + \mathbf{S}^{+} * \left(|\overline{\ddot{x}}_d|.^{\wedge 2} - |\overline{\ddot{x}}_i|.^{\wedge 2}\right) \tag{4.6}$$

4.6 Simulation Implementation

4.6.1 Adjusting for Calculated Negative Autospectrum values

When calculating response from Eqn. (4.5), at some frequency lines the mathematics calculated a negative autospectrum, which is not physically realizable. For those frequencies, the voltage autospectrum was just set to a small positive value. Theoretically, the mathematical calculations show that the pseudo-inverse could achieve a very good match to the desired acceleration autospectra. This can be seen in Fig. 4.7 in the left plot of the sum of the PSDs. However, this requires the negative voltage autospectra which are not achievable. When the negative voltage autospectra are set to a small positive number, the result on the right is achieved, which is an over-prediction. Figure 4.4 indicates that the over-prediction is reduced with the Tikhonov regularization.

4.6.2 Degree of Tikhonov Regularization and Associated Benefit

For the Tikhonov pseudo-inverse, the authors chose the constant c to be 0.01 times the largest element on the diagonal of the $\mathbf{S}^T\mathbf{S}$ matrix. The condition number of the S matrix is shown in Fig. 4.8, with and without this regularization. The regularization results in 2 orders of magnitude improvement of the condition number which helps ensure that the pseudo-inverse does not "blow up" producing unachievable voltage inputs. Regularization is known to degrade the accuracy of the solution slightly with the benefit of not destroying the solution due to an inversion based on noise in the signals.

In Fig. 4.9 is displayed a voltage time history input for each of the six shaker amplifiers based on the pseudo-inverse with and without regularization. The dark blue plot is the required input voltage time history without the Tikhonov regularization and the red plot shows the reduced voltage time history associated with the Tikhonov regularization. The largest difference is a factor of four in RMS voltage, to obtain almost the same acceleration PSD results.

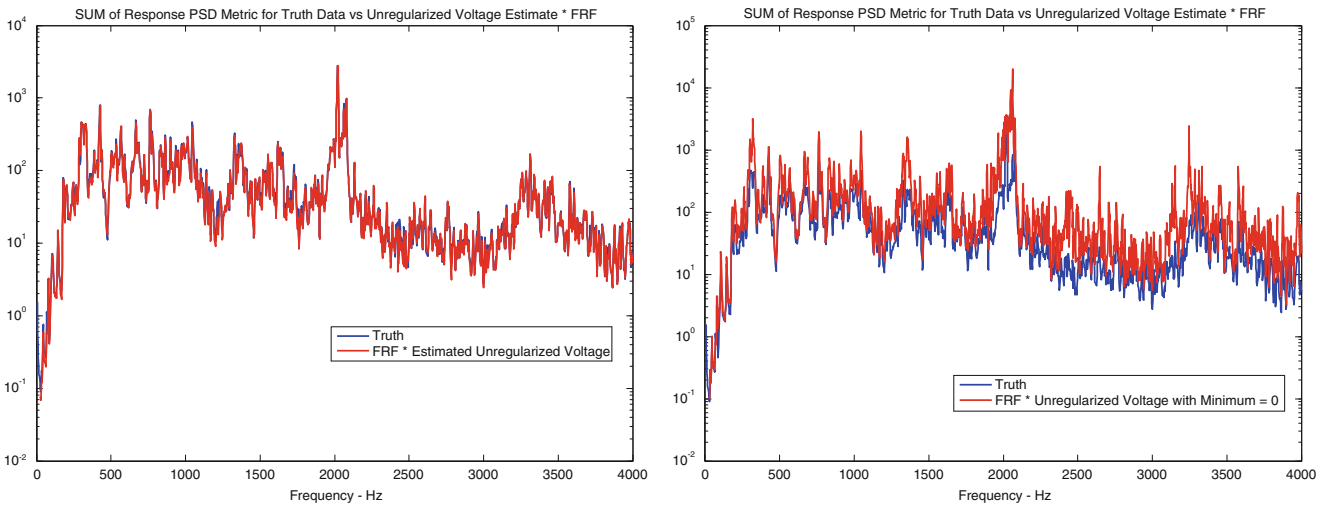

Fig. 4.7 Mathematical prediction of sum of acceleration PSDs. Result with some negative autospectra (*left*)—result with all autospectra positive (*Right*)

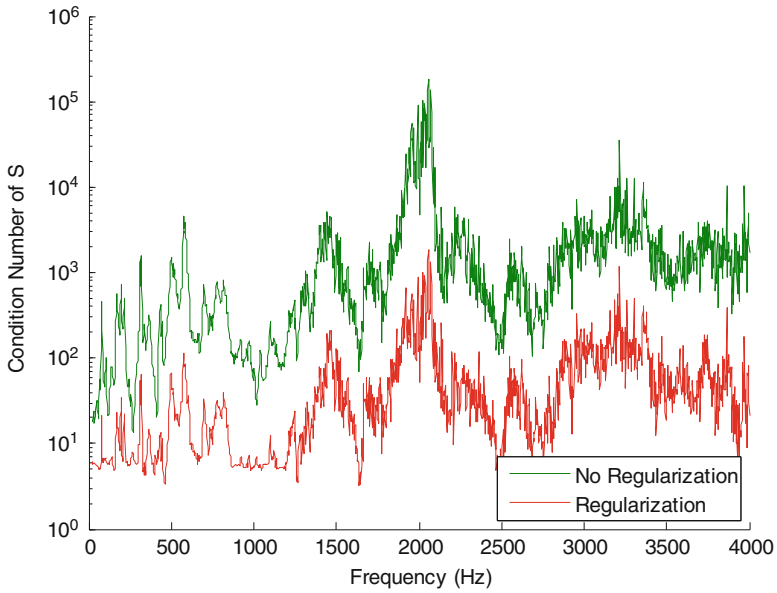

Fig. 4.8 Condition number of the S matrix with and without regularization

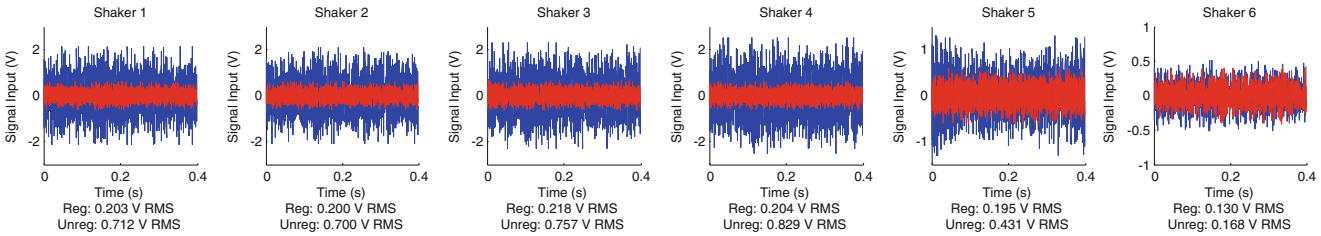

Fig. 4.9 Comparison of voltage input time histories required without regularization (*blue*) and with regularization (*red*)

4.6.3 Mathematical Results with a Decreased Number of Control Accelerometers

In many realistic cases, the number of available target accelerometers may be much less than the 37 used in this research. For a typical industrial system, the shaker voltage might have to be predicted from only a dozen measured responses. The authors randomly picked 12 of the 37 gages to determine the voltage inputs and then compared that result for the sum of all 37 PSDs for another environment in Fig. 4.10. In most frequency bands, the match of the result calculated from only 12 gages looks amazingly good. One region of error is circled.

4.6.4 Calculation of the Voltage Input Time Histories

Voltage time histories had to be generated to produce the shaker forces. After calculating the anticipated voltage autospectra from Eqn. (4.6), the square root of the ratio of the desired voltage autospectrum and initial voltage autospectrum at a particular frequency line was used to scale the initial amplitude of the sine wave of the particular frequency line. The phase of the corresponding sine wave was set randomly. This was performed independently for each source signal, so no two shakers had correlated phases. One frame of data would be constructed from this sum of sine waves with random phase. The next frame would be constructed from the same amplitude sine waves each with a new random phase. Hundred frames were utilized to give many frames whose voltage values were uncorrelated in phase for our assumption that the voltage inputs from one shaker to another were uncorrelated. On subsequent iterations we did not let the voltage at a specific line change more than $+100$ %, -67 %. In hindsight, the first iteration using the Tikhonov regularization could probably be allowed to change to $+$anything and -90 %, and further iterations could have tighter bounds.

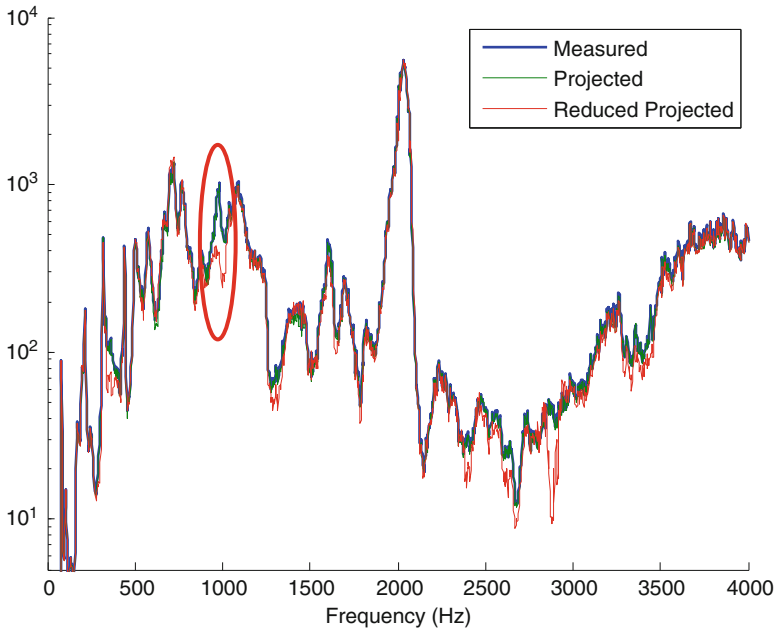

Fig. 4.10 Sum of 37 PSDs from some measured data (*blue*), mathematical prediction from voltage calculated using all 37 responses (*green*), mathematical prediction from voltage calculated using 12 responses (*red*)

4.7 Research to Increase Shaker Force

After the simulation was performed, interested parties wished to know the maximum force we could have put into the test article. Force inputs for the vibration simulation were from 19.8 to 49 N rms for the six shakers, which is about 25–65 % of the shaker rated force capability (225 N). The rms power delivered by the shakers was extremely low, 0.35 W for the shaker which required the most power. The questions that followed were: (1) Could we increase the force input beyond the rated shaker capability; and (2) What was the force capability of the connecting hardware?

4.7.1 MB50 Shaker Capabilities to 4000 Hz

Some testing with flat random voltage inputs was done with the shakers up to 4000 Hz that showed the shakers could deliver three times the rated force capability if the power required was not beyond the capability of the amplifier. The shakers could put out peak forces of 675 N. At massive "hard points" the shaker could put out more force than at non-massive "soft locations". At the soft locations, the velocity was so high that the power capability of the amplifier (force times velocity) was exceeded.

4.7.2 Stinger Force Capability

In considering the force capability of the shaker and connecting hardware, the authors decided that the connecting hardware should provide protection for the shaker and test hardware. This required understanding the force capability of the connecting hardware and developing a failure mechanism that would protect the shaker and test unit. It was decided that having the stinger slip under its setscrews was an inexpensive way to protect the expensive shaker and test article from costly failure. The force gage would also be protected if the stinger slipped below the maximum rated force capability of the force gage and its connecting stud. Static tests were performed on the stinger attached to a receptacle with either one or two size #3 setscrews and torques on the setscrews from 0.228 to 0.8 N-m. 0.8 N-m would begin to deform the threads in the aluminum stinger receptacle to receive the set screw. In Fig. 4.11 is given the static force at which the stinger slipped for several trials of set screw torque for one or two set screws. Having two screws torqued to 0.6–0.7 N-m would allow the maximum 675 N capability of the MB50 shaker to be utilized.

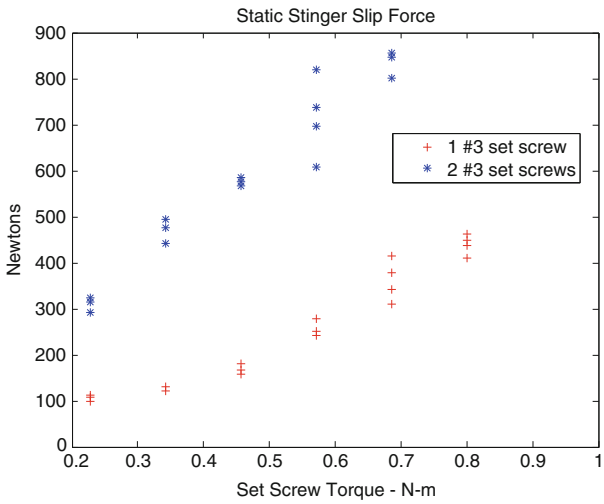

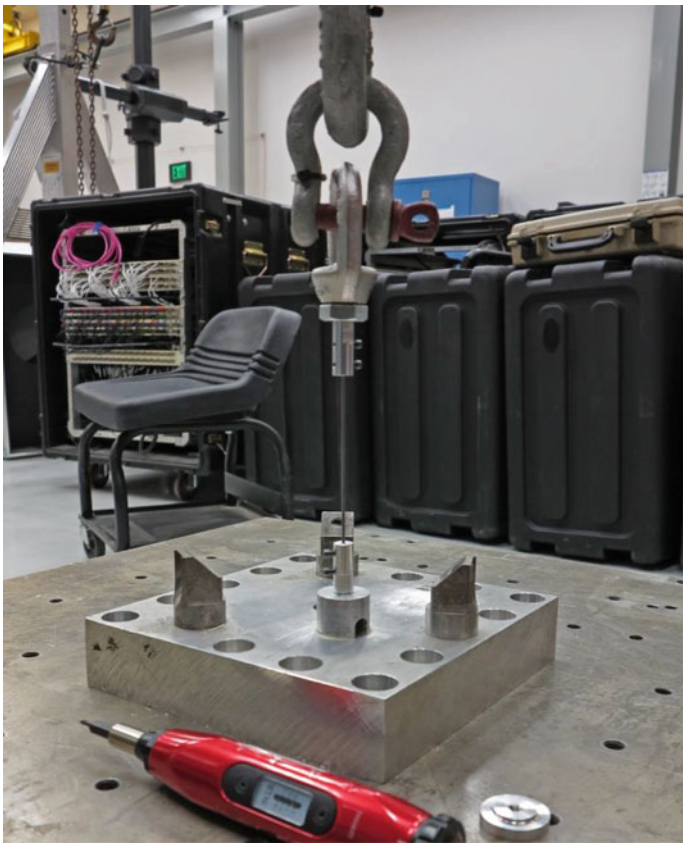

Fig. 4.11 Static stinger slip force vs. set screw torque

4.7.3 Force Capability of Cap

The cap to which the force gage is attached (see Fig. 4.2) was attached to a flat surface with Durakore brand dental cement and pulled to failure while measuring the static force that caused the dental cement to fail. Wide variability in the dental cement failure strength was found for the 200 mm^2 attachment area. If the surface was smooth and not cleaned well, the dental cement could fail as low as 200 N force. With roughed up surfaces well cleaned on both sides, the failure values were above 2800 N, which is considerably above the 675 N capability of the MB50.

4.7.4 Optimal Shaker Placement and Increasing Tikhonov Regularization **c** *Value to 0.1*

Since the final responses measured indicated that the mathematical calculations for the sum of PSDs metric was almost accurate, some mathematical calculations were performed examining changing the Tikhonov regularization value, c, in Eqn. (4.4). It was found that almost the same accuracy could be obtained by increasing the value of c to 0.1. Also, the calculation was made with the FRFs gathered from six shakers mounted to the belly of the structure as in Fig. 4.1. Figure 4.12 shows the calculated match of the sum of PSDs. With these adjustments, the maximum shaker force required for any of the shakers was about 23 N rms. Using three sigma clipping, and the 675 N shaker peak force capability found in Sect. 7.1, the MB50 shakers could put out about ten times more force than required for this physical simulation, which would equate to roughly a factor of 100 in power. Of course this assumes no significant nonlinearity in the structure.

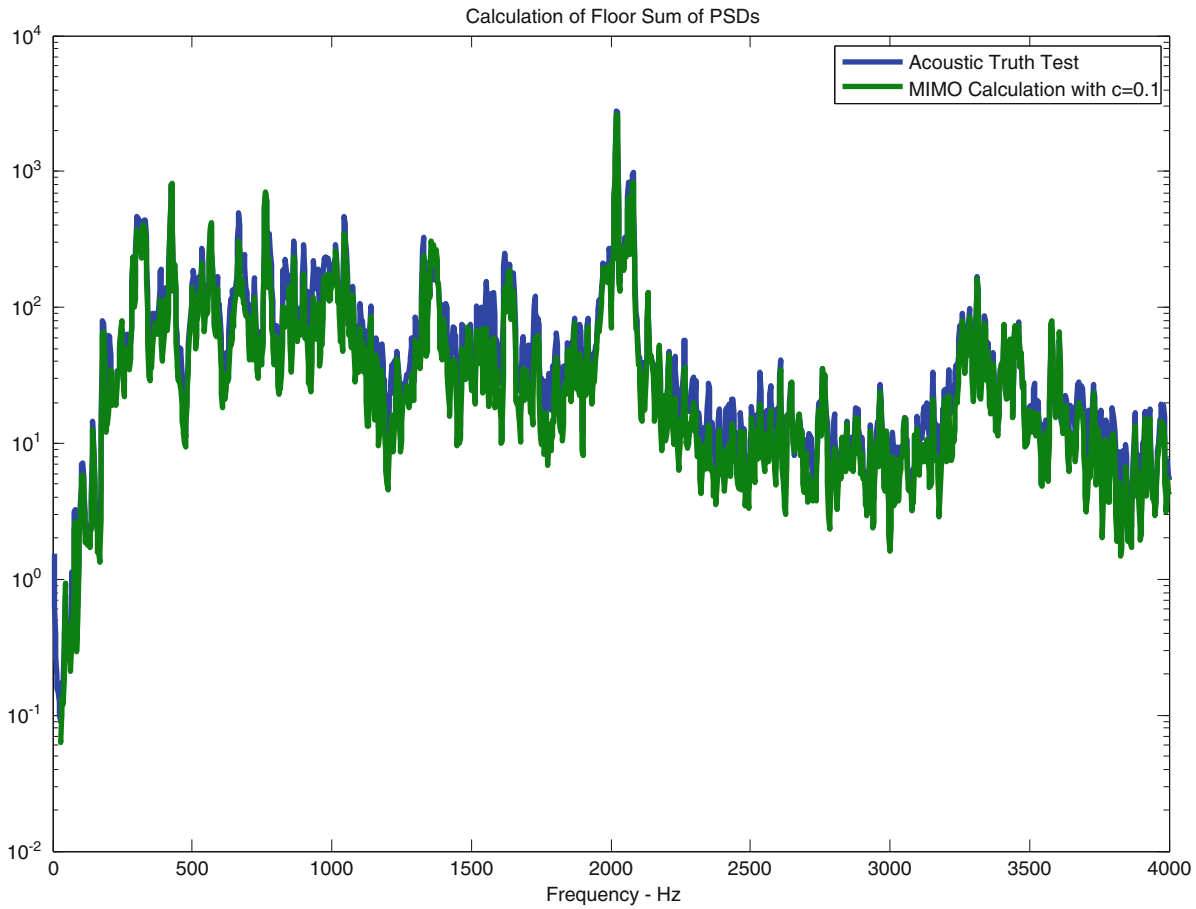

Fig. 4.12 Calculated sum of PSDs match for 6 floor mounted shakers and Tikhonov c value of 0.1

4.8 Conclusions

The six shaker input simulation was able to nearly replicate the results of an acoustic test environment up to about 3500 Hz. The match from 3500 to 4000 Hz was not very good. The element by element square of the absolute value of the FRF matrix was used with the target acceleration autospectra to calculate six voltage autospectra used for the input voltage to the shaker amplifiers in the inverse problem. Tikhonov regularization was utilized to reduce these inputs. Cross spectra were not needed for this method. Reduction of the force requirement was achieved by increasing the Tikhonov constant without a significant reduction in accuracy of matching the 37 internal target acceleration responses. The inverse problem was also calculated for 12 of the original 37 target autospectra with only a small reduction in accuracy of the simulation. Some additional reduction in the required forces appeared available based on the location of the shaker attachment. For the 4000 Hz bandwidth, it was found that the shakers could produce about three times the rated force input when attached to hard points of a structure. At soft structural force connection locations, the maximum force was limited by the amplifiers in the cases we tested. The slip force of the stingers and set screws was characterized to provide a degree of protection for the shakers and the test article.

Acknowledgments The acoustic test was performed by Eric Stasiunas and Ryan Schultz. Anthony Gomez was the primary technologist involved in the data acquisition along with the authors. Jerry Cap was the prime motivator who was able to get the testing programmed and funded. Diane Callow provided a huge portion of the logistic support in terms of writing the test plan and getting the testing approved to meet the operational and safety requirements. Bill Fladung from ATA engineering showed us how to input user defined time histories into the VTI source modules.

References

1. Himelblau, H., Hine, M.J.: Effects of triaxial and uniaxial random excitation on the vibration response and fatigue damage of typical spacecraft hardware. In: Proceedings of the 66th Shock and Vibration Symposium, Arlington, 1995
2. Daborn, P.M., Roberts, C., Ewins, D.J., Ind, P.R.: Next-generation random vibration tests. In: Proceedings of the 32nd International Modal Analysis Conference, paper number 92, Orlando, February 2014
3. Daborn, P.M., Ind, P.R., Ewins, D.J.: Replicating aerodynamic excitation in the laboratory. In: Proceedings of the 31st International Modal Analysis Conference, paper number 42, Garden Grove, 2013